ISPRS Journal of Photogrammetry and Remote Sensing 146 (2018) 124–136

Contents lists available at ScienceDirect

ISPRS Journal of Photogrammetry and Remote Sensing

journal homepage: www.elsevier.com/locate/isprsjprs

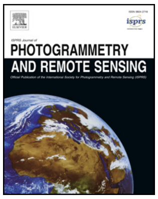

UAV-based multispectral remote sensing for precision agriculture: A comparison between different cameras

Lei Deng[a,b], Zhihui Mao[a,*], Xiaojuan Li[a], Zhuowei Hu[a,b], Fuzhou Duan[a,b], Yanan Yan[a]

[a] *College of Resource Environment and Tourism, Capital Normal University, Beijing 100048, China*
[b] *Spatial Information Technology Engineering Research Center of MOE, Beijing 100048, China*

ARTICLE INFO

Keywords:
Multispectral camera
Unmanned Aerial Vehicle (UAV)
Remote sensing
Vegetation index
SPAD value

ABSTRACT

Unmanned aerial vehicle (UAV)-based multispectral remote sensing has shown great potential for precision agriculture. However, there are many problems in data acquisition, processing and application, which have stunted its development. In this study, a narrowband Mini-MCA6 multispectral camera and a sunshine-sensor-equipped broadband Sequoia multispectral camera were mounted on a multirotor micro-UAV. They were used to simultaneously collect multispectral imagery and soil–plant analysis development (SPAD) values of maize at multiple sampling points in the field, in addition to the spectral reflectances of six standard diffuse reflectance panels with different reflectance values (4.5%, 20%, 30%, 40%, 60% and 65%). The accuracies of the reflectance and vegetation indices (VIs) derived from the imagery were compared, and the effectiveness and accuracy of the SPAD prediction from the normalized difference vegetation index (NDVI) and red-edge NDVI (reNDVI) under different nitrogen treatments were examined at the plot level. The results show that the narrowband Mini-MCA6 camera could produce more accurate reflectance values than the broadband Sequoia camera, but only if the appropriate calibration method (the nonlinear subband empirical line method) was adopted, especially in visible (blue, green and red) bands. However, the accuracy of the VIs was not completely dependent on the accuracy of the reflectance, i.e., the NDVI from Mini-MCA6 was slightly better than that from Sequoia, whereas Sequoia produced more accurate reNDVI than did Mini-MCA6. At the plot level, reNDVI performed better than NDVI in SPAD prediction regardless of which camera was employed. Moreover, the reNDVI had relatively low sensitivity to the vegetation coverage and was insignificantly affected by environmental factors (e.g., exposed sandy soil). This study indicates that UAV multispectral remote sensing technology is instructive for precision agriculture, but more effort is needed regarding calibration methods for vegetation, postprocessing techniques and robust quantitative studies.

1. Introduction

In recent years, precision agriculture has become a frontier area of agricultural science that has attracted great attention worldwide (Zhang et al., 2016). Maize is a major grain crop around the world and plays a vital role in ensuring food security. Phenotype refers to the external characteristics of an organism, such as the shape, structure, size and color, which are collectively determined by the genotype and environmental factors (Sadras et al., 2013). Under various environments, extracting the phenotypic information of maize accurately and rapidly is important for monitoring crop growth to ensure food security, ecological safety and sustainable agricultural development (Liebisch et al., 2015).

Two types of methods are available for extracting phenotypic information of crops: manual and remote sensing methods. The former directly measure phenotypic data, such as the biomass, leaf area index (LAI) and chlorophyll content [often represented by the measured soil–plant analysis development (SPAD) value] (Yamamoto et al., 2002). Most manual methods require the instrument operators to perform intensive field collection and are therefore destructive and effort and time consuming. In contrast, remote sensing methods are advantageous in that they can cover large areas and are nondestructive means for phenotypic crops (Yang et al., 2017). Numerous researchers have used satellite-based remote sensing methods to study maize, soybeans and winter wheat. For example, Moderate Resolution Imaging Spectroradiometer multi-time series vegetation indices (VIs) have been used to investigate crop yields, traits and growth conditions during various phenological stages (Sakamoto et al., 2010, 2013). High-accuracy LAI values have been estimated using VIs, such as the optimized

---

* Corresponding author.
E-mail addresses: denglei@cnu.edu.cn (L. Deng), 2160902134@cnu.edu.cn (Z. Mao).

https://doi.org/10.1016/j.isprsjprs.2018.09.008
Received 19 March 2018; Received in revised form 1 September 2018; Accepted 6 September 2018

soil-adjusted VI (OSAVI) and the modified triangular VI extracted from Compact High Resolution Imaging Spectrometer imagery (Liang et al., 2015). However, in precision agriculture, the low spatial resolution of satellite remote sensing makes it unsuitable for plot-level applications, which enable effective reduction of the effects of field variability to increase the genetic signal-to-noise ratio. Furthermore, plot-level phenotypic information of maize may be important for assessing crop performance under different conditions and provide significant guidance for breeding (Zaman-Allah et al., 2015). In addition, the influence of background factors, such as soil, at the plot level cannot be ignored (Liebisch et al., 2015). Consequently, to meet the high spatial resolution real-time continuous monitoring requirements of precision agriculture (Hanya et al., 2010), some alternative approaches are demanded.

In recent years, unmanned aerial vehicles (UAVs) have increased in prominence due to their advantages (e.g., high flexibility, ease of operation, high spatial resolution and acquisition of data on demand). Therefore, UAVs provide a new technical means for extracting phenotypic information of crops in fields rapidly and nondestructively. Significant progress have been made in UAV-based phenotype extraction, such as VI generation, LAI and SPAD prediction, and carotenoid estimation in vegetation leaves using hyperspectral imagery (Liu et al., 2016; Yang and Everitt, 2012; Yang et al., 2004; Zarco-Tejada et al., 2016). Remarkable results have also been achieved in using thermal infrared (IR) sensors and light detection and ranging (LiDAR) technology to measure vegetation canopy temperatures and heights and to estimate biomass, chlorophyll and nitrogen (N) contents at different times (Andujar et al., 2013; Berni et al., 2009; Maimaitijiang et al., 2017). These studies have demonstrated that the above techniques are valuable for precision agriculture; however, all these sensors (hyperspectral, LiDAR and thermal IR) are expensive and too heavy for UAVs, and the data acquired from them are difficult to process and analyze. Although consumer-level digital camera-based visible light sensors are easy to operate, inexpensive, and can be utilized in agriculture (Baresel et al., 2017), they are inadequate for more in-depth research and applications due to their lack of red-edge (RE) and near-IR (NIR) bands, which are highly sensitive bands used for vegetation monitoring. In contrast, multispectral sensors can easily be used to acquire high spatial resolution (centimeter-level) multiband (from the visible to the NIR) remote sensing data, thus achieving a balance between cost and usability. Table 1 presents the main parameters of multispectral cameras commonly used in precision agriculture.

In terms of bandwidth, multispectral cameras can be divided into two categories: narrowband and broadband. Narrowband means that the spectrum range is small (Sampson et al., 2003). As can be observed from Table 1, Mini-MCA6 is a typical narrowband camera with a bandwidth of 10 nm. Generally, with a smaller spectral range, more accurate spectral measurements can be obtained (Imai, 2000). Broadband cameras have wide spectral ranges (e.g., Sequoia has a bandwidth of 40 nm), which are usually similar to those of satellites; consequently, it is straightforward to apply some algorithms (e.g., for VIs) used for satellite-based sensors to data from broadband cameras (Fernández-Guisuraga et al., 2018). However, it should be noted that the results derived from narrowband and broadband cameras are not in complete agreement or even conflict (Zhao et al., 2007).

In addition to bandwidth, radiometric calibration is another important factor determining spectral accuracy and reflectance-based derivatives (e.g., VIs). Before using multispectral imagery, radiometric calibration is a prerequisite and a key step, in which the digital number (DN) value recorded by the camera can be converted into the spectral reflectance. Two radiometric calibration methods are often employed for UAV-based multispectral remote sensing, that is, preflight calibration and vicarious calibration (Dinguirard and Slater, 1999). The former procedure, used to characterize the camera (e.g. Sequoia), provides the necessary laboratory-calibrated parameters, such as the absolute radiometric calibration coefficients. Regarding vicarious calibration, the empirical line method is one of the commonly used methods, which depends on accurate characterization of reference scenes/targets whose reflectance can be determined during the UAV flight (Liu et al., 2018; Turner et al., 2014). For Mini-MCA6, only DN values can be obtained if no vicarious calibration is performed. In short, these two calibration methods represent two typical scenarios for multispectral cameras usage, i.e., Mini-MCA6 is a typical narrowband multispectral camera that uses vicarious calibration, whereas Sequoia is broadband camera that uses preflight calibration. Therefore, it is very valuable and necessary to compare the accuracy, applicability and potential of different types of sensors and different calibration methods in precision agriculture.

In view of these issues, the main objective of this paper is to compare the ability of narrow- and broadband multispectral cameras in precision agriculture. In particular, it was examined whether the two types of cameras differ regarding their ability to provide high-accuracy remotely sensed data and derivatives under different circumstances. In this context, the study addresses the following research questions: (1) What are the effects of bandwidth and different calibration methods on the accuracy of the spectral reflectance values? (2) What is the relationship between the accuracy of the absolute reflectance and the VI(s)? (3) Which of the broadband and narrowband VIs have advantages in obtaining crop physicochemical parameters? To this end, a narrowband (Mini-MCA6) and a broadband (Sequoia) multispectral camera mounted on a multirotor UAV were used to acquire high spatial resolution multispectral data. By comparing these multispectral data with ground-measured data, the accuracies of the spectral reflectance values obtained using different calibration methods were compared, and the prediction accuracies for SPAD values under different N treatments from different VIs were analyzed. Finally, the applicability of UAV-based multispectral remote sensing technology to precision agriculture is discussed.

Table 1
Main parameters of some commonly used multispectral cameras.

Multispectral sensor	Spectral range (nm)/Central wavelength (band width) (nm)	Resolution (pixels)	Weight (g)	GSD@50 m (cm)
Sentera Quad	RGB Red: 655 (40)Red edge: 725 (25) NIR: 800 (25)	1248 × 950	170	1.10
ADC Micro	Green: 520–600 Red: 630–690 NIR: 760–900	2048 × 1536	200	1.90
Buzzard	Blue: 500 (50) Green: 550 (25) Red: 675 (25) NIR1: 700 (10) NIR2: 750 (10) NIR3: 780 (10)	1280 × 1024	250	2.21
MiniMCA6	Blue: 490 (10) Green: 550 (10) Red: 680 (10)Red edge: 720 (10) NIR1: 800 (10) NIR2: 900(20)	1280 × 1024	700	2.70
XNiteCanon SX230 NDVI (modified)	Blue: 385–470 Green: 500–570 NIR: 670–770	4000 × 3000	223	3.00
RedEdge	Blue: 475 (20) Green: 560 (20) Red: 668 (10)Red edge: 717 (10) NIR: 840 (40)	1280 × 960	150	3.40
Sequoia (MS)	Green: 550 (40) Red: 660 (40) Red edge: 735 (10) NIR: 790 (40)	1280 × 960	72	4.70